Transition Probabilities for the $5s'[1/2]_1$-$3p$ Transitions of Ne I†*

S. Inatsugu and J. R. Holmes
Department of Physics and Astronomy, University of Hawaii, Honolulu, Hawaii 96822
(Received 12 March 1973)

Transition probabilities for nine allowed transitions between the $5s'[1/2]_1$ and $3p$ states of neon have been measured in side light emission from a discharge tube placed inside a He-Ne-laser radiation field. The laser was tunable at nine visible lines belonging to the $5s'[1/2]_1$-$3p$ array. The gas mixture and the discharge current were adjusted so as to obtain a transparent plasma at the respective laser wavelength. Such a plasma is characterized by an absence of both resonance absorption and stimulated emission, creating a condition that $N_1/N_2 = g_1/g_2$ between the upper- and the lower-energy levels of the laser transition. This condition immediately enables the intensity ratio of two transitions arising from two different energy levels to be reduced to the ratio of the transition probabilities. The relative A values were put into an absolute scale using Bennett and Kindlmann's lifetime data on $3p$ levels. Nine independent measurements were made through the use of nine laser transitions. Excellent agreement was seen between these independent measurements. The estimated error in the relative measurements is 2%, and the best value of the absolute $A_{632.8}$ was found to be $(0.339 \pm 0.014) \times 10^7\,\mathrm{s}^{-1}$ When compared with the data of Hansch *et al.* and Bychkova *et al.*, who employed a similar method but only one laser transition at 632.8 nm, significant disagreement is seen. It was found that the self-absorption of $3p$-$3s$ lines is as large as 20%. Argon was added to reduce this effect to a negligible level. There is strong evidence that this effect was disregarded in other measurements, thereby resulting in the large disagreement with our data.

I. INTRODUCTION

Despite the importance of the neon $3s_2$-$2p_4$ transition (the Paschen notation will be used throughout the following text) at 632.8 nm in the He-Ne laser, very few experimental works[1-3] have reported measuring the radiative transition probabilities connected to this transition. In particular, the uncertainty of the measured values is reported as large as 20–30%. The $3s_2$ state of Ne I lies rather high above the ground state, and the spectra originating from this level range from vacuum uv to infrared. The resonant self-absorption of the uv line and the complexity of the detector arrangements make it unrealistic to measure relative A values and normalize through the lifetime of the level.

The method used in this experiment is very similar to the ones used by Hansch and Toschek,[1] Bychkova *et al.*,[2] and others.[3,4] A laser is used as a resonance lamp to illuminate an absorption cell containing a discharge of a gas under investigation. The discharge tube was placed inside the laser optical cavity in order to make use of the full strength of the cavity field. In such an arrangement, the lower-energy state need not be a ground state or metastable state as in the case of a conventional resonance absorption technique. An intense laser field interacts strongly with the pair of energy levels in resonance, perturbing the populations of these energy-level pairs selectively. The amount of perturbation is effectively detected in the changes of the intensities of the spontaneous side light components emitted from these levels. It is possible to adjust the discharge conditions of the absorption cell in such a way that there is neither absorption nor stimulated emission of the line in resonance. At this moment the net interaction ceases to exist between the laser field and the plasma; the plasma is "transparent" to the laser radiation. This condition can be determined very accurately by detecting "null," when the intensity change in the side light components vanishes. Such a transparent plasma will render a constraint between the populations of the energy levels in resonance, such that

$$N_1/N_2 = g_1/g_2 , \tag{1}$$

where N_i is the population and g_i is the statistical weight of the state. A direct comparison of two emission intensities of spectra originating from different energy levels does not provide a relative transition probability unless a good knowledge of populations of the levels is available. In this experiment, however, Eq. (1) immediately removes this difficulty. The intensity ratio I_1/I_2 in this case may be written as

$$\frac{I_1}{I_2} = \frac{A_1 N_1 h\nu_1}{A_2 N_2 h\nu_2} = \frac{A_1 g_1 \lambda_2}{A_2 g_2 \lambda_1} , \tag{2}$$

where A_i is an absolute transition probability, $h\nu_i$ is photon energy, and λ_i is wavelength. Intensity

I_i is given in units of [photon energy/sec]. Since wavelengths and statistical weights are known, the ratio of transition probabilities, A_1/A_2, is readily obtained if the intensity ratio is determined experimentally.

We believe that this method deserves a further development in both theory and experimental technique, since it has potentially a wide applicability in measuring transition probabilities between excited states high above the ground states of various elements. Because of the more direct approach and fewer assumptions, systematic errors are intrinsically smaller with this method. Since many laser oscillations have become available fairly routinely in various elements, the scope of this method is no longer limited.

II. RATE-EQUATION ANALYSIS

The schematic levels of Ne I are shown in Fig. 1(a). Nine laser oscillations are possible between $3s_2$ and nine of the ten $2p$ levels (the transition to $2p_9$ is forbidden). The wavelengths of these transitions are given in the second column of Table II. In order to illustrate the model used in the rate-equation analysis below, consider energy levels $3s_2$ and $2p_1$. They are denoted by $|1\rangle$ and $|2\rangle$, respectively, and shown in Fig. 1(b). In a low-pressure glow discharge, the populations of energy levels attain a steady state through detailed balancing of excitation and deexcitation mechanisms. If a strong semimonochromatic radiation field $\rho(\lambda)$ (a laser field at $\lambda = 730.5$ nm in this particular case) is applied from an external source and allowed to interact with levels $|1\rangle$ and

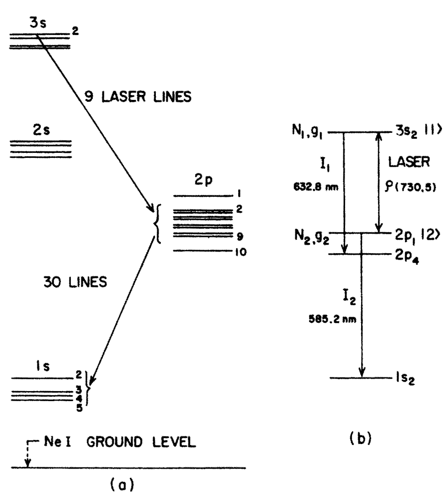

FIG. 1. (a) Schematic energy-level diagram of Ne I. (b) One of the nine sets of neon transitions and energy levels directly involved in the rate-equation analysis. Paschen notation is used.

$|2\rangle$, the steady-state rate equation for level $|1\rangle$ may be written as

$$0 = dN_1/dt = -N_1W_1 - \rho(\lambda)(B_{12}N_1 - B_{21}N_2) + R_1, \quad (3)$$

and if the field is removed from the plasma,

$$0 = dN_1'/dt = -N_1'W_1 + R_1, \quad (4)$$

where N_1 and N_1' are the populations of level $|1\rangle$ when the laser field is on and when the laser field is off, respectively; W_1 is the total deexcitation coefficient of level $|1\rangle$; R_1 is the rest of the processes, which are assumed unaffected by the presence of the laser field (this assumption is valid since the correction term due to collisional excitation from level $|2\rangle$ is negligibly small, and eventually it will vanish when the plasma becomes transparent); and B_{ij} is the induced transition probabilities between levels $|1\rangle$ and $|2\rangle$. Taking the difference between Eqs. (3) and (4) yields

$$\Delta N_1 W_1 = -\rho(\lambda)(B_{12}N_1 - B_{21}N_2), \quad (5)$$

where $\Delta N_1 = N_1 - N_1'$. Similarly, for the state $|2\rangle$, one may obtain

$$\Delta N_2 W_2 = \rho(\lambda)(B_{12}N_1 - B_{21}N_2) + C\Delta N_1. \quad (6)$$

The additional term $C\Delta N_1$ is introduced in order to include explicitly the contribution due to the direct and indirect cascading from level $|1\rangle$. The deexcitation coefficient W_i includes such processes as the radiative decay and the collisional relaxation by electrons, ions, and ground-state atoms. Thus, rate equations (3) and (4) are exact to the extent of the assumption that R_i remains unchanged by the field. If the discharge condition is adjusted by varying the gas composition and the current density in such a way that the plasma becomes totally transparent to the laser radiation, the interaction ceases to exist. Difference terms ΔN_1 and ΔN_2 in Eqs. (5) and (6) vanish at this moment, and both equations reduce to the following exact equation:

$$B_{12}N_1 - B_{21}N_2 = 0. \quad (7)$$

Equation (1) immediately results from Eq. (7), since $B_{12}/B_{21} = g_2/g_1$. The transparency condition may be determined by monitoring spontaneous side light emissions I_1 and I_2 arising from levels $|1\rangle$ and $|2\rangle$, respectively. Since I_i is linearly proportional to N_i, $\Delta I_i = 0$ verifies the condition that $\Delta N_i = 0$. The ratio I_1/I_2 measured at this juncture will determine the relative transition probability of these two emission lines via Eq. (2). A new set of energy levels and an appropriate laser line is selected and the same procedure is repeated. Altogether nine such measurements can be made since there are nine different laser transitions. The $3s_2-2p_4$ transition at 632.8 nm was chosen for I_1 throughout the experiments. As for I_2, one from every group of $2p-1s$ transitions (see the first column of Table I) with a common upper level is judiciously chosen for each set of energy levels and a laser line. Thus, in effect, A values of these lines were determined with respect to $A_{632.8}$.

III. APPARATUS

The most essential part of the experiment was to make available a He-Ne laser that was capable of lasing at the entire nine wavelengths in $3s_2$-

TABLE I. Summary of relative transition probabilities $A_{ps}/A_{632.8}$, and procedures of normalization to obtain the absolute value $A_{632.8}$. A_{ps} is an A value of a $2p$-$1s$ transition and $A_{632.8}$ is the A value of the $3s_2$-$2p_4$ transition at 632.8 nm.

Transitions	λ(nm)	$A_{ps}/A_{632.8}$ [a]	$\sum_s(A_{ps}/A_{632.8})$ [b]	$\sum_s A_{ps}=\tau^{-1}$	$A_{632.8}$ (10^7 sec^{-1})
$2p_1$ -$1s_4$	540.056	0.265		6.95 [c]	0.3410 [c]
s_2	585.249	20.118	20.383	(7.15) [d]	(0.3508) [d]
$2p_2$ -$1s_5$	588.190	3.379			
s_4	603.000	1.654			
s_3	616.359	4.319		5.31	0.3279
s_2	659.895	6.844	16.195	(5.19)	(0.3205)
$2p_3$ -$1s_4$	607.434	17.783		5.69	0.3184
s_2	665.209	0.0867	17.869	(5.86)	(0.3279)
$2p_4$ -$1s_5$	594.483	3.345			
s_4	609.616	5.342		5.23	0.3359
s_2	667.828	6.883	15.570	(5.22)	(0.3353)
$2p_5$ -$1s_5$	597.553	1.035			
s_4	612.845	0.196			
s_3	626.650	7.346		5.02	0.3351
s_2	671.704	6.403	14.980	(5.13)	(0.3426)
$2p_6$ -$1s_5$	614.306	8.317			
s_4	630.479	1.228		5.07	0.3453
s_2	692.947	5.137	14.681	(5.01)	(0.3413)
$2p_7$ -$1s_5$	621.728	1.879			
s_4	638.299	9.470			
s_3	653.288	3.192		5.03	0.3332
s_2	702.405	0.557	15.098	(5.02)	(0.3325)
$2p_8$ -$1s_5$	633.443	4.761			
s_4	650.653	8.839		5.04	0.3489
s_2	717.394	0.846	14.446	(5.10)	(0.3530)
$2p_9$ -$1s_5$	640.225	...	...	5.15 (5.06)	...
$2p_{10}$-$1s_5$	703.241	7.472			
s_4	724.517	2.759			
s_3	743.890	0.682		4.04	0.3690
s_2	808.246	0.0355	10.949	(3.78)	(0.3452)
				$\langle A_{632.8}\rangle_{av}$ =	0.3394 [e] (0.3389) [f]

[a] Statistical errors were less than 1%. Estimated systematic error 2%, except for 665.2- and 808.2-nm lines, where it is 5%.

[b] Estimated uncertainty 2%.

[c] Figures without parentheses are based on Bennett and Kindlmann's (Ref. 10) lifetime experiments.

[d] Figures given in parentheses are based on Bridges and Wiese's (Ref. 9) relative emission experiments.

[e] Error on the average value is 1.4%. The standard deviation of the individual $A_{632.8}$ is 4.2%.

[f] Error on the average value is 1%. The standard deviation of the individual $A_{632.8}$ is 3.2%. Better consistency is seen with the values given in parentheses.

$2p_i$ transitions, including the 632.8-nm line, and whose oscillations could be tuned individually at a single wavelength. As reported by various authors,[5-7] laser oscillations were observed at all of the nine transitions. We constructed two aluminum cold cathode lasers with 4-mm-bore Pyrex tubing, one having 1-m discharge length and the other 1.5 m. Both lasers were provided with Brewster windows and a stopcock. The tubes were filled with He^3 and Ne^{20} in the ratio of 6.5 to 1, at a total pressure of 1.3 Torr. This composition of the gas was found experimentally to yield maximum gain for the weaker lines towards the yellow and green regions.

As shown in Fig. 2, the cavity configuration of our laser was very much similar to the ones described in Refs. 5 and 6, in which use was made of one or two full-dispersion Brewster-angle quartz prisms. Spherical mirrors of radius 2 m were placed at an angle of minimum deviation for the region of the wavelengths of the laser lines. Three sets of mirrors, dielectric coated for maximum reflectivity, were necessary in order to cover the entire nine laser lines; the wavelengths of the coating were 540, 620, and 730 nm, each corresponding to laser oscillations at 543.4, 593.9–640.1, and 730.5 nm, respectively. The cavity configuration was of long radius so as to excite off-axis transverse modes deliberately in order to fill the doppler-gain profile as much as possible. The selection of the individual laser line was accomplished by adjusting the tilt of the mirror located closer to the prism, while the other mirror was held fixed. The intracavity prism may also be useful in suppressing the multiple-path gain of the 3.39-μ oscillation, but it cannot quench the single-path gain or the so-called superradiance effect. This effect was reduced to a negligible level when a string of permanent magnets was placed along the full length of the discharge. It was observed that some weaker lines stopped lasing when the magnets were removed from the discharge. When the second set of mirrors coated for 620 nm were in use, there were as many as four neighboring lines oscillating simultaneously at one setting of mirror tilt. This fact made it necessary to employ the second prism in tandem in order to separate out three red lines at 629.3, 632.8, and 635.1 nm.

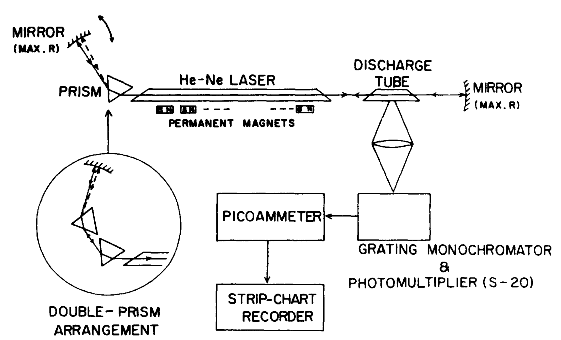

FIG. 2. Experimental setup. The double-prism arrangement as shown in the circle was used to separate the 629.3-, 632.8- and 635.2-nm lines. The direction of observation and the electric vector of the laser field lie in the same plane.

The discharge tube, containing the gas to be studied, was placed at the farthest end of the prism as shown in the figure. The discharge tube was made of Pyrex tubing having 4-mm-bore diameter, 1-mm wall thickness, and 4-cm discharge column. It was provided with Brewster windows, an aluminum cold cathode, and a vacuum stopcock. While it was in the laser cavity it was separated from the vacuum station. After each measurement the tube was evacuated down to 10^{-8}-Torr range before the next gas filling, in order to ensure freedom from any possible gas contamination. The laser and the discharge tube were excited by two separate high-voltage regulated dc power supplies. An optimum laser tube current varied for different laser lines; its value was approximately 10 mA for the green line, 18 mA for yellow lines, and 28 mA for the rest of the lines. The discharge tube was operated typically at a current below 10 mA. The detail of the gas composition and the discharge conditions for the transparent plasma will be described in Sec. IV.

The central portion of the discharge plasma was focused on the entrance slit of the Jarrel–Ash $\frac{1}{2}$-m grating monochromator. The direction of the observation was parallel to the electric field vector of the laser field. An anisotropy of the spontaneous radiation pattern due to the alignment of the radiating atoms along the optical field is of no importance since when the plasma becomes transparent to the laser field, no net interaction exists between the radiating atoms and the field; thus $\Delta I_i = 0$ in any direction of the observation. The detection was made by an EMI 9558A photomultiplier tube (S-20 response) and its photocurrent was measured by a Keithley model 417 picoammeter. The lens–monochromator–photomultiplier-tube system was calibrated against a quartz iodine standard lamp, whose absolute calibration was within 5%. The relative response, however, could be calibrated to as good as 1% when the spectral line separation was less than 100 nm. The photomultiplier tube was selected for a low dark current and was operated at a room temperature. Intensities of the emissions were strong for most of the lines and an excellent signal-to-noise ratio was obtained. This fact eliminated the use of phase-sensitive detection, which was originally considered.

IV. EXPERIMENTS

To determine the optimum gas mixture of the discharge tube, the following experiment was performed in the experimental setup as shown in Fig. 2. With the laser tuned to 611.8 nm($3s_2 - 2p_6$), intensity changes ΔI_1 and ΔI_2 were monitored in the spontaneous-emission side light components at 632.8 nm ($3s_2 - 2p_4$) and 630.5 nm ($2p_6 - 1s_4$), respectively. The discharge tube was filled with a He^3 and Ne^{20} mixture at 1.5 Torr. The neon partial pressure was varied from 0.05 to 1.3 Torr. The measurements were made at various discharge currents between 2 and 12mA. In Fig. 3, the curves of ΔI_1(632.8 nm) at 2 and 12 mA are plotted against neon partial pressure. As clearly seen in this figure, ΔI_1 vanishes at neon partial pressure between 0.8 and 1.1 Torr for a discharge current ranging from 2 to 12 mA. The plasma becomes transparent when $\Delta I_1 = 0$. When ΔI_1 is positive the lower laser level is more populated so that a net absorption of the laser light takes place, and when ΔI_1 is negative a population inversion is created. Notice that the maximum population inversion occurs at a helium-neon mixture ratio of 7 to 1 approximately.

Owing to the levels $1s_{3,4,5}$ being metastable, the spectral lines terminating on these levels are partially self-absorbed. Also, the $1s_2$ level behaves like a metastable state under the gas-pressure range of this experiment, because the uv radiation connecting the ground level is completely trapped. The effect of self-absorption is proportional to the A value of the spectral line. The intensity ratio of a strong to a weak line may be decreased under the presence of self-absorption. In the $2p - 1s$ transitions of neon, it was found that some strong-line intensities were decreased as much as 20% under a discharge condition similar to this experiment. This effect is demonstrated in Fig. 4. Four spontaneous emissions belonging to the $2p_7 - 1s$ transition group were measured at various neon partial pressures while the total pressure of the He^3 and Ne^{20} mixture was kept constant at 1.5 Torr. The discharge current was set at 5 mA throughout. The 702.4-nm line ($2p_7 - 1s_2$) was taken as the reference to evaluate the relative transition probabilities of the three other lines. Since the $1s_2$ level would be less

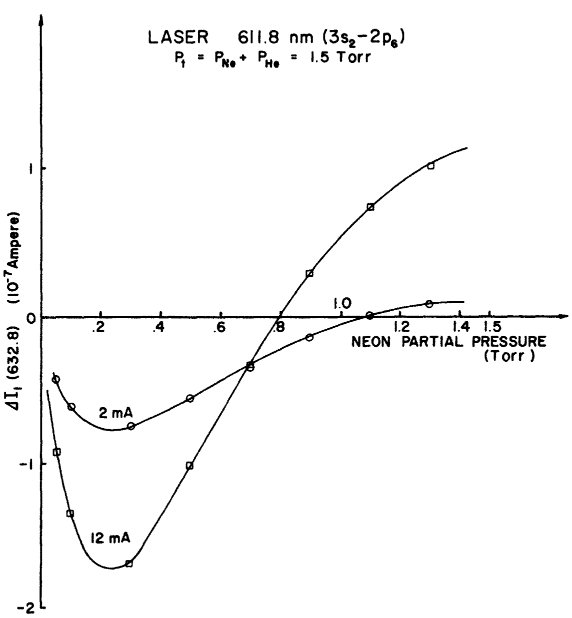

FIG. 3. Intensity change ΔI_1 of the 632.8-nm spontaneous-emission line vs neon partial pressure. The laser field at 611.8 nm perturbed the populations of the $3s_2$ and $2p_6$ levels. The total gas pressure of He^3 and Ne^{20} was held constant at 1.5 Torr. The plasma becomes "transparent" at the neon partial pressure between 0.8 and 1.1 Torr as the discharge current is varied from 12 to 2 mA.

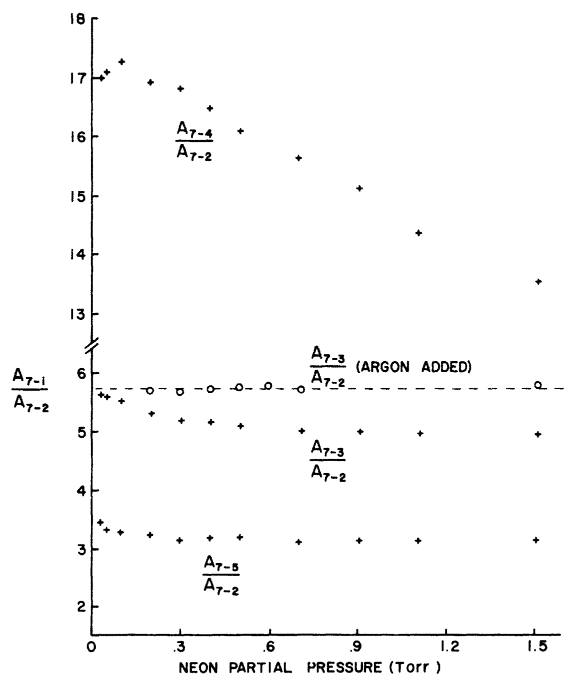

FIG. 4. Effect of self-absorption on the apparent relative A values of some neon lines terminating on $1s$ metastable levels. A_{7-2} ($2p_7$-$1s_2$ transition at 702.4 nm) is taken as a reference. Measurements were taken in the side light emission from a discharge tube containing a He-Ne mixture at 1.5 Torr. Discharge current was 5 mA. Addition of argon into the discharge removes the self-absorption effect as shown by a dotted line.

metastable than the other $1s$ states and the A value of the 702.4-nm line (denoted by A_{7-2} in Fig. 4) happens to be relatively small compared with the other A values in this group (denoted by $A_{7-3,4,5}$), this line is expected to be least affected by the self-absorption effect. As clearly seen in Fig. 4, the "apparent" relative A value varies as a function of neon partial pressure. For example it is decreased at least 15% from the true value at a neon partial pressure of 1.0 Torr, at which the plasma becomes transparent according to Fig. 3. Hence, a significant amount of systematic error would result in the relative A values unless this effect is eliminated. Such an effect indeed could be avoided if the plasma is optically thin, or the metastable state populations are rapidly destroyed. It should be noticed further that in Fig. 4, the relative A value increases as neon partial pressure is reduced. Collisions with the ground-state helium atoms effectively destroy these metastable $1s$ states. Such a collisional destruction mechanism is more dominant than the collisions with the container wall, since the mean free path between atom-atom collisions is estimated to be 0.1 to 0.2 mm at 1.5 Torr while the discharge tube diameter is 4 mm. Collisions with the ground-state neon atoms, however, do not contribute to the deexcitation since the resonant-transfer-excitation effect repopulates the $1s$ states after collisions. Thus, in the zero-neon-partial-pressure limit, a true relative A value may be obtained because the lifetime of the $1s$ metastable states will be effectively reduced, and at the same time the total neon particle density becomes small enough to yield an optically thin plasma.

The collisional deexcitation of the neon $1s$ states will be more effectively carried out by hydrogen[8] or argon[9] atoms instead of helium. We added 0.1 Torr of argon to the He-Ne mixture while the total pressure was maintained at 1.5 Torr. The result for A_{7-3}/A_{7-2} is shown by circular points in Fig. 4. Notice these points fall on a straight line (a dotted line) throughout the pressure range of this experiment, and it is in a very close agreement (within 1%) with that obtained by zero-pressure extrapolation. The effect of argon was the same for the rest of the emission lines of the $2p-1s$ transition array. We believe that the presence of the argon continuum in the vicinity of the neon $1s$ metastable levels is responsible for the effective destruction of these states. Although the emission intensity of all lines became somewhat weak owing to the addition of argon, a similar inversion characteristic, as seen in Fig. 3, was still preserved except that the emissions are now free from self-absorption.

The detection of the plasma transparency and the comparisons of intensity components I_1 and I_2 were conducted in the following manner. The discharge tube was filled with a He-Ne-Ar mixture at a total pressure ranging from 0.8 to 1.4 Torr, of which argon partial pressure occupied 0.1 Torr always. The rest was a mixture of He^3 and Ne^{20} at the ratio of 1 to 2 approximately. The discharge was run about five minutes or longer for the tube to reach equilibrium. The monochromator slits were set at 25 μ. First, I_1 (632.8-nm emission) was monitored with the laser radiation "on." The output of the picoammeter was continuously recorded on the strip-chart recorder. The laser field was then blocked to see if there was any change in the intensity (ΔI_1) on the chart trace. If there was a change, the discharge current was adjusted slightly and the same procedure was repeated until there was no observable change of the recorder trace. The minimum discernible amount of the change on the recorder was approximately $\frac{1}{4}$% of the full scale in the most unfavorable situation. The "null" condition was created at the discharge current of 5 mA or less. If the current exceeded 5 mA, a new gas filling was sought for in order to keep the current below 5 mA. This was one of the precautionary measures to ensure the absence of self-absorption. Once the null was detected on I_1, the emission from the lower level, I_2, was selected and the same null detection procedure was repeated to see if there was any residual intensity change which might have eluded detection. This entire procedure was then repeated ten times on the average over the same pair of energy levels. When the particular set of energy levels $3s_2$ and $2p_4$ was under investigation, the detection of the null was impaired by presence of the scattered laser light at 632.8 nm caused by the discharge tube walls. This problem, however, was alleviated by monitoring the 611.8-nm line instead, as well as the line from the lower laser level. In selecting the lines to be monitored among the numerous possibilities, the first preference was placed upon such lines that terminated on the $1s_2$ level. If such a line were too weak or too remote from the 632.8-nm line, the second preference was placed on those lines with medium strength terminating on other than the $1s_2$ level, and located near the 632.8-nm spectrum. This was another precautionary measure to avoid self-absorption (if any) and the calibration error of the detector spectral response.

V. RESULTS AND DISCUSSION

The relative A values for $2p$ - $1s$ transitions with respect to $A_{632.8}$ were obtained and are listed as $A_{ps}/A_{632.8}$ in the third column of Table I. The error is estimated to be 2% except for extremely weak lines such as 665.2 and 808.2-nm lines, where it is 5%. It is interesting to compare the results with those obtained by Hansch[1] and Bychkova[2] at this stage. Only one laser (632.8 nm) was used in their experiments so that there is only one relative value, $A_{609.6}/A_{623.8}$, available for the comparison. The value for $A_{609.6}/A_{632.8}$, according to their results, is 4.71 and 3.36 respectively, while it is 5.34 in our data. The differences of 12 and 31% respectively, below our value may well be attributed to the self-absorption of the 609.6-nm line, since the absorption is strong in this particular line.

We proceeded to convert relative values into the absolute scale using the well-established lifetime data by Bennett and Kindlmann,[10] the uncertainty of which is claimed to be 1–3%. The relative values are summed within the group sharing the same upper level, and presented in column 4 of Table I. The absolue transition-probability-sums according to Bennett *et al.* are shown in column 5 without parentheses. The absolute value of $A_{632.8}$, therefore, may be calculated by dividing column 5 by column 4. This yields nine independent $A_{632.8}$ values as shown in column 6 without parentheses. The best value for $A_{632.8}$ is found to be $(0.3394 \pm 0.0048)\times 10^7$ sec^{-1}, the uncertainty being 1.4%, a considerably large portion of which was added by the ninth $A_{632.8}$ deviating greatly from the rest. The values given in parentheses are based on the recent emission experiments by Bridges and Wiese,[9] who performed relative measurements over the entire $2p-1s$ array assuming a local thermodynamics for the $2p$ levels. Their relative values were normalized to the total transition probability sum by Bennett and Kindlman.[10] Although the data set of Bridges and Wiese does not provide an independent check for the absolute scale of $A_{632.8}$, it can provide an independent crosscheck for our data's consistency, since their relative values are obtained entirely in a different manner. In fact their relative values are proved to be more consistent with the j-file sum rule and through other extensive comparisons than Bennett and Kindlmann's data.[9] Thus one may consider the transition probability sums given in parentheses to be an improved version of Bennett and Kindlmann's data. The best value for $A_{632.8}$ was found to be $(0.3389 \pm 0.0035)\times 10^7$ sec^{-1}, the uncertainty being only 1%.

The measurements were highly repeatable and all the statistical errors became less than 1% at 1 standard deviation after 5 to 10 runs. The null detection was very sensitive and the error was less than a few percent for a single measurement in the worst situation. The sensitivity of the null-detection method can be estimated in the following manner. Consider Eq. (5), which is exact if $\triangle N_1$ is small. Solving for N_2/N_1, and after simple algebra, one obtains

$$\frac{\triangle(N_2/N_1)}{(N_2/N_1)_0} = \frac{\triangle(I_2/I_1)}{(I_2/I_1)_0} = \frac{\triangle(A_{ps}/A_{632.8})}{A_{ps}/A_{632.8}} = \frac{W_1}{\rho B_{12}} \frac{\triangle I_1}{I_1}, \tag{8}$$

where

$$(N_2/N_1)_0 = B_{12}/B_{21} = g_2/g_1 ,$$

$$\triangle(N_2/N_1) = N_2/N_1 - (N_2/N_1)_0 ,$$

and

$$\triangle(I_2/I_1) = I_2/I_1 - (I_2/I_1)_0 .$$

Equation (8) was checked experimentally by plotting $\triangle(I_2/I_1)/(I_2/I_1)_0$ vs $\triangle I_1/I_1$. To obtain this plot the discharge current was varied about the point where the null was found. For a given gas mixture, W_1 is insensitive to a small change of the discharge current so that the plot should exhibit a straight line with a slope $W_1/\rho B_{12}$. Using the 611.8-nm laser, the slope was found to be 0.8 and no tendency of deviation from a straight line was noticed for $\triangle I_1/I_1$ as large as 10%. In this case 1% of a null-detection error will result in 0.8% error in the relative A value, $A_{ps}/A_{632.8}$, for a single measurement. In the actual experimental situation, however, the error component I_1 on the chart trace was discernible to even less than $\frac{1}{4}$% of the full scale in the most unfavorable case, which amounts to 0.2% error in $A_{ps}/A_{632.8}$. According to an order-of-magnitude estimation, this slope corresponds to the lifetime of the $3s_2$ level being $\simeq 30$ nsec, including collisional deexcitation (this value is reasonable since the uv-trapped radiative lifetime is 62 nsec according to Klose[11]), if one assumes the laser flux density inside the cavity to be $\simeq 10$ W/cm^2 with an oscillation bandwidth $\simeq 1$ GHz at the wavelength 611.8 nm. The laser field of the yellow and green lines was weaker than the rest. In this case the slope $W_1/\rho B_{12}$ would become greater by an order of magnitude, and a $\frac{1}{4}$% change in $\triangle I_1/I_1$ would result in 2 to 3% error in $A_{ps}/A_{632.8}$ for a single measurement. It was noticed during the measurement that the null was more ambiguous when these laser lines were in use. Actual error, however, was still less than 1% for 10 runs.

Considering all the error factors including the self-absorption effect and the detector spectral response calibration, the total error included in the relative values $A_{ps}/A_{632.8}$ is 2%, except for some weaker lines such as the 665.2- and 808.2-nm lines, where it is 5%. The error on the best value of $A_{632.8}$ was found to be only 1%. However, in presenting its absolute figure an additional 3% systematic error should be added to it in order to include the error in Bennett and Kindlmann's lifetimes. Thus we present the absolute transition probability of the 632.8-nm line ($3s_2-2p_4$) in Ne I to be $(0.339\pm0.014)\times10^7$ sec^{-1}.

With an additional relative-intensity measurement of the $3s_2-2p_i$ lines, we were able to obtain the complete set of the absolute transition probabilities including the rest of the nine allowed transitions. The results are shown on Table II along with the results of Hansch and Toschek,[1] Bychkova *et al.*,[2] and Decomps and Dumont.[12] One may easily notice rather extensive disagreement between our data and those from Refs. 1 and 2 despite the similarity of the experimental method. The reason for such disagreement, as discussed earlier in this section, is primarily because of the self-absorption of the 609.6-nm ($2p_4-1s_4$) line. The third data of Decomp and Dumont[12] were obtained by Hanle-effect measurement, which is based on an entirely different principle, and their result agrees with ours excellently. It is unfortunate that the values for the other lines are not available in this data set for comparison. The relative A values for the rest of the lines should be obtainable with good accuracy, since the transitions arise from the same upper level. When normalized to our value of the 632.8-nm line, however, large disagreement is seen among some of the data; especially those of Ref. 2 are in poor agreement, while data of ours and Ref. 1 are in good agreement, except for the 543.4-nm line. Such relative A-value measurements had been performed previously in our laboratory by Lilly and Holmes[3] and their results are in good agreement with our present results throughout. Their absolute values, however, were calculated in terms of one of the values obtained by Hansch and Toschek,[1] which we have here found laden with rather excessive errors. In view of improved accuracy of our current measurements, the corresponding A values of the $3s_2$ - $2p_i$ transitions given in Ref. 3 should be superseded by the results of this experiment as given in column 3 of Table II.

The current results also confirm the conclusion drawn by Lilly and Holmes[3] that LS and jl coupling models are not adequate for describing the $3s_i$ - $2p_j$ transitions of Ne I. On the other hand, these nine transitions will complete one of the four files of the neon $2p^55s$ - $2p^53p$ transition array, so that we may use the j-file sum rule of Shortley[13] to evaluate the radial transition integral σ^2 for this array. Such a sum rule is applicable to an array of transitions defined by two upper and lower energy-level configurations with quantum numbers nl and $n'l'$, and it is independent of the actual coupling scheme of angular momenta. It can be shown for the $5s\to3p$ ($l\to l'=l+1$) transitions ($3s\to2p$ in Paschen notations) that

$$\sum_p S_{sp}=(2J_s+1)(l+1)(2l+3)\sigma^2=3(2J_s+1)\sigma^2\,, \qquad (9)$$

where the line strength S_{sp} is related to the tran-

TABLE II. The absolute transition probabilities for the $3s_2$-$2p_i$ transitions of Ne I.

Transitions	λ (nm)	This expt.	Hansch and Toschek (Ref. 1)	(10^6 sec^{-1}) Bychkova *et al.* (Ref. 2)	Decomps and Dumont[a] (Ref. 12)
$3s_2$-$2p_1$	730.483	0.255	0.37		
$2p_2$	640.107	1.39			
$2p_3$	635.185	0.345	0.52	0.70	
$2p_4$	632.816	3.39	5.1	6.56	3.24
$2p_5$	629.374	0.639		1.35	
$2p_6$	611.801	0.609	0.93	1.28	
$2p_7$	604.613	0.226	0.39	0.68	
$2p_8$	593.931	0.200		0.56	
$2p_9$	forbidden				
$2p_{10}$	543.365	0.283	0.52	0.59	
Estimated errors		4%	14–21%[b]	17–24%[b]	19%

[a] This experiment was based on the Hanle-effect measurements, while the others used the same method as described in the text.

[b] These two data sets were based on one laser line at 632.8 nm, and the value of $A_{609.6}=23.8\times10^6$ sec^{-1} (Ladenberg, Ref. 8) was used to convert relative values to absolute values. The error included in this value, which is 30%, is not included in the error estimations given here.

sition probability by the relationship

$$S_{sp} = (2J_s + 1)3h\lambda^3 A_{sp}/64\pi^4. \tag{10}$$

And finally we are able to obtain from our data on Table II that

$$\sum_p S_{sp}/(2J_s + 1) = 0.913 = 3\sigma^2, \tag{11}$$

or $\sigma^2 = 0.304$ (atomic units), which is in excellent agreement with the value $\sigma^2 = 0.31$ predicted from the Coulomb approximation.[14] This is the first time that the validity of the Coulomb approximation was tested for the $5s$ - $3p$ transition array of Ne I.

VI. CONCLUSIONS

An experimental method of measuring transition probabilities of spectral lines belonging to two different upper levels has been described in detail. The method is based on the availability of a laser transition between these two levels. The interaction of the laser field with these excited energy states enables verification and detection, in the side light emission from a discharge tube, of a condition of the plasma that is characterized by its being transparent to the laser radiation. The sensitivity of the "null" detection was found to be extremely high, being proportional to the laser-radiation flux density. The method was then used to measure the transition probability of the 632.8-nm ($3s_2$ - $2p_4$) line in Ne I in relation to the transition probabilities of $2p$ - $1s$ lines. Nine independent measurements were obtained by making use of all nine laser oscillations arising from the $3s_2$ level. The uncertainty of such relative values is estimated to be 2%. They were converted into an absolute scale through Bennet and Kindlmann's lifetime measurements as well as Bridges and Wiese's improved transition probability sums. The latter set was used mainly to crosscheck our relative transition probability sums. Nine $A_{632.8}$ values were consistent and the best value was found to be $(3.39 \pm 0.14) \times 10^6$ sec^{-1}. The uncertainty is 4% including systematic errors. Using this value, the rest of the $3s_2$ - $2p$ transition probabilities were obtained by normalizing the relative measurements. The result was compared with other experiments by Hansch and Toschek and Bychkova *et al.*, and agreement was found to be poor. Such disagreement is partly due to the less accurate value of $A_{609.6}$ used to normalize their relative values. It was also pointed out that a significant self-absorption effect was evidenced in the other measurements.

Although the primary scope of this experiment was to measure $A_{632.8}$ in relation to the known A values of some of the $2p$ - $1s$ transitions, we have linked up, in effect, the A values of the entire set of transitions (except for 640.2-nm line) arising from different $2p$ levels by measuring all the relative values, $A_{ps}/A_{632.8}$. This is significant since the procedure does not involve measurements of any thermodynamic parameters like plasma temperature and particle density of excited states, nor involve absolute intensity measurements. It is only necessary to create a transparent plasma and perform relative intensity measurements. An error in this type of a measurement is minimal because of its intrinsic freedom from many of the nagging systematic errors and certain assumptions. These relative values in turn could be renormalized to an absolute scale using the accurate $A_{632.8}$ value resulting from this experiment. The detailed account of this is beyond the scope of this paper and will be published elsewhere.

We believe that the application of the method described here is not restricted to the particular set of the energy levels we treated here, but it can be readily extended to other energy levels in neon, as well as those in other gases. An immediate candidate may be the $3s_2$ - $3p$ and $2s$ - $2p$ transitions of Ne I, where numerous laser oscillations have been observed. Work is presently underway to investigate these transitions. We suggest that a strong continuously tunable organic-dye laser may be useful where an appropriate laser oscillation is difficult to obtain for the particular set of energy levels under investigation.

ACKNOWLEDGMENT

The authors would like to thank E. M. Kaczorowski for his valuable technical assistance.

---

†Work partially supported by grants from Air Force Office of Scientific Research and Research Corporation.

*Work based in part on a dissertation submitted by S. Inatsugu in partial fulfillment of the requirements for the Ph.D. degree at the University of Hawaii.

[1]T. Hansch and P. Toschek, Phys. Lett. **20**, 273 (1966).

[2]T. V. Bychkova, V. G. Kirpilenko, S. G. Rautian, and A. S. Khaikin, Opt. Spektrosk. 22, 674 (1967).

[3]R. A. Lilly and J. R. Holmes, J. Opt. Soc. Am. **58**, 1406 (1968).

[4]J. H. Parks and A. Javan, Phys. Rev. **139**, A1351 (1965).

[5]A. L. Bloom, Appl. Phys. Lett. **2**, 101 (1963).

[6]A. D. White and J. D. Rigden, Appl. Phys. Lett. **2**, 211 (1963).
[7]D. L. Perry, IEEE J. Quantum Electron. QE–7, 102 (1971).
[8]R. Ladenberg, Rev. Mod. Phys. **5**, 243 (1933).
[9]J. M. Bridges and W. L. Wiese, Phys. Rev. A **2**, 285 (1970).
[10]W. R. Bennett, Jr. and P. J. Kindlmann, Phys. Rev. **149**, 38 (1966).
[11]J. Z. Klose, Phys. Rev. **188**, 45 (1969).
[12]B. Decomps and M. Dumont, IEEE J. Quantum Electron. **QE–4**, 916 (1968).
[13]G. H. Shortley, Phys. Rev. **47**, 295 (1935).
[14]D. R. Bates and A. Damgaard, Philos. Trans. R. Soc. Lond. A **242**, 101 (1950).